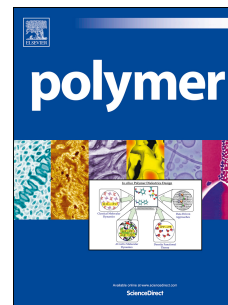


Journal Pre-proof

Efficient thiazole-based polyimines as selective and reversible chemical absorbents for CO₂ capture and separation: Synthesis, characterization and application

Elaheh Akbarzadeh, Abbas Shockravi, Vahid Vatanpour



PII: S0032-3861(19)30846-8

DOI: <https://doi.org/10.1016/j.polymer.2019.121840>

Reference: JPOL 121840

To appear in: *Polymer*

Received Date: 26 June 2019

Revised Date: 26 August 2019

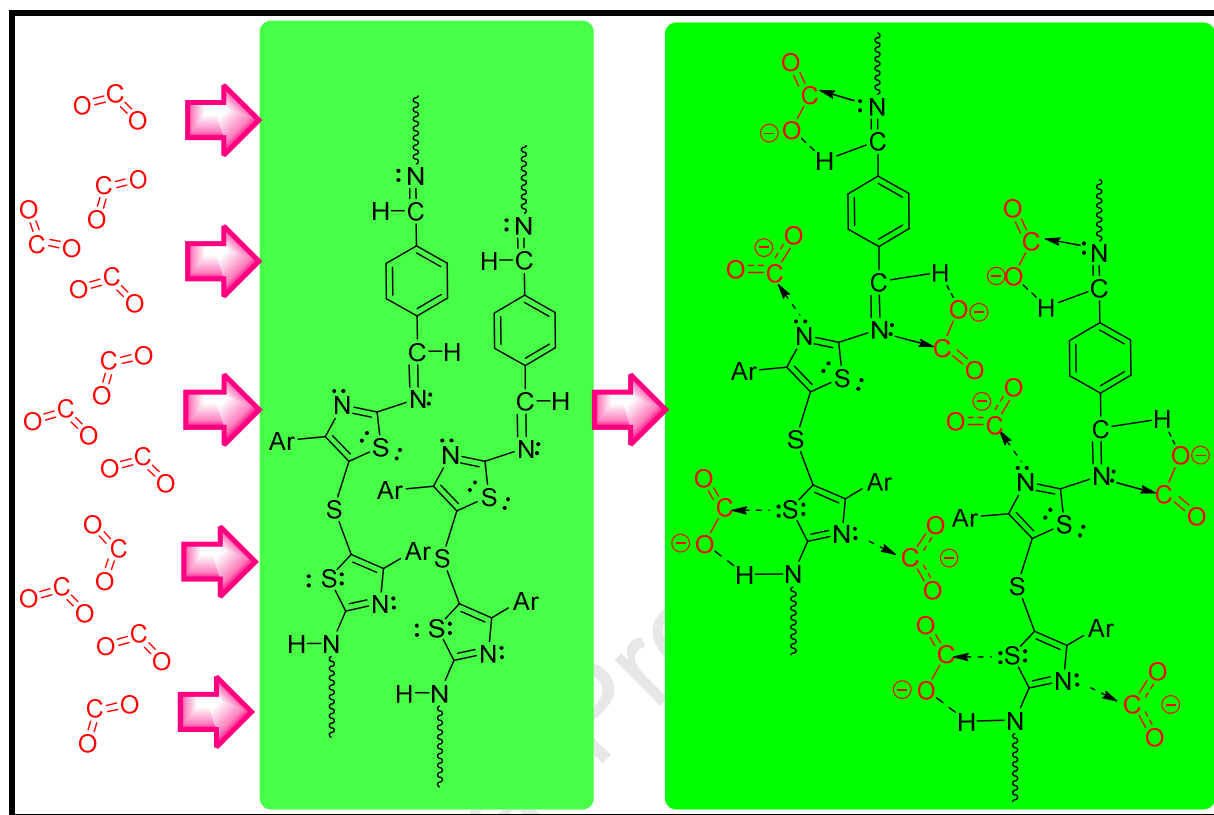
Accepted Date: 24 September 2019

Please cite this article as: Akbarzadeh E, Shockravi A, Vatanpour V, Efficient thiazole-based polyimines as selective and reversible chemical absorbents for CO₂ capture and separation: Synthesis, characterization and application, *Polymer* (2019), doi: <https://doi.org/10.1016/j.polymer.2019.121840>.

This is a PDF file of an article that has undergone enhancements after acceptance, such as the addition of a cover page and metadata, and formatting for readability, but it is not yet the definitive version of record. This version will undergo additional copyediting, typesetting and review before it is published in its final form, but we are providing this version to give early visibility of the article. Please note that, during the production process, errors may be discovered which could affect the content, and all legal disclaimers that apply to the journal pertain.

© 2019 Published by Elsevier Ltd.

Graphical abstract:



Efficient Thiazole-Based Polyimines as Selective and Reversible Chemical Absorbents for CO₂ Capture and Separation: Synthesis, Characterization and Application

Elaheh Akbarzadeh,^{a,*} Abbas Shockravi^{a,*} and Vahid Vatanpour^a

^a Faculty of Chemistry, Kharazmi University, Mofatteh Avenue 49, 15719-14911 Tehran, Iran

* **Corresponding authors e-mail:** ela_akbarzadeh@khu.ac.ir;

abbas_shockravi@yahoo.co.uk; shockravi@khu.ac.ir

Abstract

A new series of polyimines (PIMs-1-9) including *ortho*-linked thiazole units and flexible thioether linkages were synthesized from diamine monomers (DA-1-3) and some commercially available aromatic dialdehydes (terephthalaldehyde, isophthalaldehyde and 2,5-thiophenedicarboxaldehyde) via Schiff-base condensation reaction. The synthesized polymers as amorphous solids were obtained with high efficiency (74-89%), inherent viscosities in the range of 0.98–1.33 dL g⁻¹ in DMF and high solubility in aprotic polar solvents (DMSO, DMAc, DMF, NMP, and Py). The PIMs were characterized via viscosimetry, elemental analysis, FT-IR spectroscopy, X-ray diffraction (XRD), Brunauer–Emmett–Teller (BET), thermogravimetric analysis (TGA) and differential scanning calorimetry (DSC). High thermal resistance revealed for PIMs as glass transition temperatures (T_g s) ranging in 104-189 °C along with 10% weight loss temperatures exceeding 268-390 °C in air and 310-430 °C in nitrogen atmosphere. The polymers were examined for CO₂ absorption at 298 K as well as 318 K and high absorption capacity exhibited (maximum 3.72 mmol g⁻¹ or 163.68 mg g⁻¹ at 1 bar and 298 K for PIM-4) after 2h and desorption at 373 K under vacuum conditions (100 mbar) in 20 min. More importantly, remarkable ideal selectivity ratios of CO₂/N₂ (77.3) and CO₂/CH₄ (13.7) at 1 bar and 298 K were obtained and recyclability of PIM-4 for CO₂ capturing was determined without considerable loss of gas absorption.

Keywords: Gas separation; CO₂ capture; Selectivity; Polyimine; Thiazole, Heterocycle

1. Introduction

Industrialization in terms of deforestation by human activities in the form of burning fossil fuels for energy beside substantial land use changes has been increased CO₂ emission which is the world's greatest environmental challenge in the atmosphere. Critical issues such as global warming trends and shifting climate patterns are consequences of increasing CO₂ levels along with other greenhouse gases [1, 2]. From other perspective, CO₂ has harmful effects in the form of corrosion in oil and gas industry on downstream process lines and equipment which makes gas sweetening process as an inevitable step [3]. For these reasons, more effective sorption materials and approaches in technologies with economic cost and high-performance features are still demanding. In recent decades, great efforts have been made to achieve this goal through solvents, sorbents and membranes [4]. Conventional amines or ammonia bases dissolved in water solution, as a mostly routine method for industrial CO₂ capturing, suffers from multiple drawbacks including energy-intensive, equipment corrosion, toxicity, solvent loss, and amine oxidative and thermal degradation [5]. To reduce amine loss and energy consumption, ionic liquids (ILs) have been applied as new alternative [6, 7], but still critical properties remain including decomposition at temperatures near the boiling point, water solubility and high viscosity which lead to gas diffusion limitation. Recently, researchers have presented solid and physical adsorbents such as zeolites [8], zeolitic imidazole frameworks (ZIFs) [9, 10], metal-organic frameworks (MOFs) [8, 11, 12], functionalized silicas [8, 13-15], silica with mixed-matrix [16-19] as CO₂ separation membrane, activated carbons [8, 20] as attractive alternatives for aqueous amine solution due to their non-corrosive and eco-friendly properties which is attributed to lower energy consumption for regeneration. They are also privileged due to their smaller energy requirements causing by lower adsorption enthalpy. However, adsorption on solid materials (chemisorption) considered more desirable vs physical adsorption (physisorption) due to their

strong covalent bonds with CO₂ and high heat of absorption. This means reduction in required regeneration energy in contrast to weak van der Waals interactions and low heat of physical adsorbents [21]. More importantly, many physical adsorbents (physisorbents) suffer from insufficient selectivity particularly in gas mixture, which cause low separation efficiency and additional CO₂ purification and cost [21, 22]. Besides, regeneration of chemical adsorbents (chemisorbents) such as solid amines, alkali metal ceramics, calcium-based adsorbents and layered double hydroxides (LDHs), are energy-consumptive and water sensitive [23]. Hence, sorbents that have high CO₂ uptake/selectivity, low cost and sensitivity towards water are still demanding. On the other hand, based on the high quadrupole moment and polarisability of CO₂, applying electronegative functionalities including nitrogen-rich sites with high selectivity such as amines [5], amides [24], imines [25, 26], thiazole [27] and thiadiazoles [28] seems more favorable in the case of CO₂ absorption. In recent years, applying imine-based covalent organic frameworks (COFs) [28-30], microporous organic polymers (MOPs) [31-34], modified micro-/mesoporous polyimine with tris(2-aminoethyl)amine [35], porous organic polymers (POPs) [36], benzimidazole-linked polymers (BILPs) [37-40], ferrocene-linked porous organic polymers (FPOPs) [41] and polymer of intrinsic microporosity [42-44] have become more prevalent alternatives for CO₂ capturing. Additionally, it is determined that the porous polymers containing sulfur and activated carbons exhibited moderate capacity for CO₂ uptake under low pressure (1 bar) conditions [45-47] and exceptionally high amounts at high pressure [48], which highlights pivotal roles of sulfur presence in adsorbent structures. Actually, most of these sorbents focused on gas storage by physisorption, due to their high surface area, free volume and heat of adsorption or may be utilized complicated monomers for the synthesis of porous polymer networks. Therefore, usage of rapid, vigorous, highly selective and reversible CO₂ sorbents with low-cost and available monomers, physicochemical stability, structural and physical

susceptibility (including flexibility, heat and water resistance) for various industry applications is still demanding. Moreover, our group recently synthesized valuable thiazole-based polyamides (PAs) [49, 50], polyimides (PIs) [51-53], and poly(amid-imide)s (PAIs) [53, 54] with thioether linkages resulted in thermal and thermo-oxidative stability, high optical transparency and solution processability for polymers. Besides, novel polyoxadiazoles were explored as highly CO₂ permselective membranes [55] and novel symmetrical bis-Schiff bases introduced [56, 57]. Therefore, we envisaged that polyimines (PIMs-1-9) containing thiazole ring would be more susceptible units for CO₂ capturing or separation due to thiazole bonds (C-S or C-N) and nitrogen rich imine linkages which make polymers more active for such purposes. To the best of our knowledge, this is the first time that three efficient functional groups of thiazole, thioether and generated imine simultaneously have been used together, as a chemical absorbent, in a polymer which can improve CO₂ uptake and selectivity (over N₂ and CH₄). However, thioether linkage can also increase flexibility and thermal resistance of the polymer which subsequently provide opportunity for more applications in industry (such as membranes). More importantly, a strategy to investigate structural comparison of polyimine chains and effects of applied dialdehydes and functional groups on monomers (NO₂, Br and naphthyl) were developed as well. In fact, the current study aims to examine the performance of new PIMs for CO₂ absorption capacity and their selectivities under ambient conditions.

2. Experimental section

2.1. Materials

3-Nitroacetophenone (MERCK), 4'-bromoacetophenone (MERCK), 2-acetylnaphthalene (SIGMA-ALDRICH), iodine (SIGMA-ALDRICH), thiourea (SIGMA-ALDRICH) and aromatic dialdehydes such as isophthalaldehyde (MERCK), terephthalaldehyde (MERCK)

and 2,5-thiophenedicarboxaldehyde (MERCK) were utilized as received. In the process of purification, lithium Bromide (LiBr, MERCK) was dried at 200 °C for 24 h under vacuum before use and *N*-methyl-2-pyrrolidone (NMP, MERCK) was distilled over calcium hydride (CaH₂) under reduced pressure. Other commercially available reagents and solvents were also used without further purification.

2.2. Measurements

The elemental analysis was performed on a Perkin Elmer 2004 (II) CHN recorder (USA) elemental analysis instrument and melting points of the diamines (DAs) by Electrothermal engineering LTD 9200 apparatus. FT-IR spectra were measured with Perkin Elmer FT Spectrum RX1 (USA) over the range 400–4000 cm⁻¹ and inherent viscosities by an Ubbelohde suspended level viscometer with a 0.5 g dL⁻¹ dimethylformamide (DMF) solution at 30 °C. ¹H NMR (300 MHz) and ¹³C NMR (75 MHz) spectra of the diamines (DAs) were obtained on a Bruker DRX 300 AVANCE spectrometer using DMSO-*d*₆ as a solvent and trimethylsilane (TMS) as the reference. The wide-angle X-ray diffraction (WAXD) patterns of the polymers were recorded on a Philips PW 1800 diffractometer using the graphite monochromatized Cu K α radiation (wavelength: 0.15401 nm) with 2θ increments of 0.08 °/s over a range of $2\theta = 4\text{--}80^\circ$ at room temperature. Glass transition temperatures (T_g) were recorded on a 2010 DSC thermal analysis (TA) instrument (METTLER TOLEDO, Switzerland) and TGAs with a Du Pont 2000 thermal analysis system (METTLER TOLEDO, Switzerland) under N₂ and air atmospheres at a heating rate of 10 °C/min. Surface areas and pore size of PIMs were undertaken using BELSORP-miniIII from the N₂ adsorption at relative pressure $P/P_0 = 0.99$ in the Brunauer–Emmett–Teller (BET) model.

2.3. Synthesis of PIMs

The PIMs were synthesized via the Schiff-base condensation reactions of diamine monomers (DA-1-3) and some dialdehydes. In a typical experiment for preparation of PIM-1, a mixture of 0.472 g (1 mmol) of 5,5'-Thiobis((2-amino-4-(3-nitrophenyl)thiazole) (DA-1), 0.134 g (1 mmol) of terephthalaldehyde, 0.174 g (2 mmol) of LiBr, and 2 mL of NMP was heated and stirred at 120 °C for 3 h, under N₂ atmosphere. After 2.0 h, the viscosity of reaction solution increased and additional amount of NMP (1 mL) was added to the reaction mixture. At the end of the polycondensation, the PIM solution was slowly poured into vigorous stirring 300 mL of methanol and resulting dark colored precipitate was thoroughly filtered off with hot water (2×100 mL) and hot methanol (100 mL). Subsequently, polymer was dried in a vacuum oven at 100 °C overnight. The yield was almost quantitative and further purification was accomplished through dissolving the PIM in NMP, filtering the polymer solution, and reprecipitating into hot methanol. The same strategy was followed for the synthesis of other PIMs.

2.4. Gas absorption measurements

The gas (CO₂, CH₄ and N₂) absorptions were determined using a laboratory setup according to a volumetric method that has been schematically shown in Figure 1. The purity of the utilized gases was determined to be CO₂: 99.5%, N₂: 99.999%, CH₄: 99.5%. To ensure removal of any moisture and any gas molecules absorbed through the air, the PIMs were degassed at 423 K in a vacuum for 24 h prior to measurement. Afterwards, the samples were cooled down to 298 K and gas was introduced into the system. During the experiment, changes in the pressure of CO₂ were measured over time. Regarding the recyclability of polymers for CO₂ capturing, they were recovered in a rotatory evaporator under 373 K and vacuum condition (100 mbar) up to 20 min and then recycled in the CO₂ absorption test. The

corresponding diagrams were plotted based on the general gas equation $PV = nRT$, wherein the P , V and T represent pressure (atm), volume (L) and absolute temperature (K) respectively; n (g mol^{-1}) is the number of moles of gas and $R = 0.0821$ ($\text{L atm mol}^{-1} \text{K}^{-1}$) is ideal gas constant. The experiments were accomplished under 1 bar at 298 K and $V = 12.82$ cm^3 , in which volume totally considered as sample volume of the exhaust valve and sample tank.

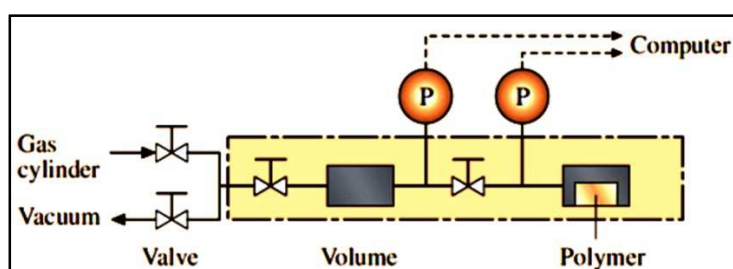
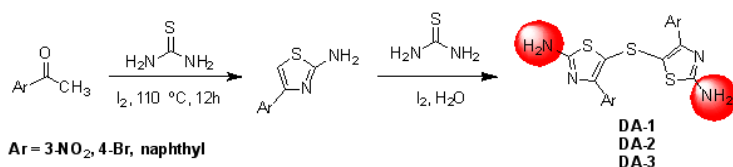


Figure 1. Setup of CO₂ uptake and selectivity tests.

3. Results and discussion

3.1. Monomer synthesis and characterization

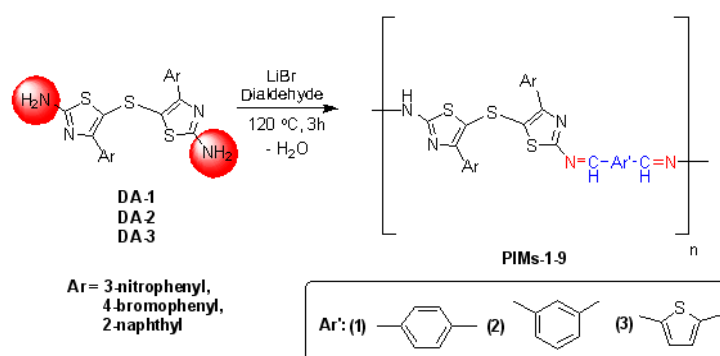
Thiazole-containing aromatic diamines 5,5'-Thiobis((2-amino-4-(3-nitrophenyl)thiazole) (DA-1), 5,5'-Thiobis((2-amino-4-(4-bromophenyl)thiazole) (DA-2) and 5,5'-Thiobis((2-amino-4-(naphthalen-2-yl)thiazole) (DA-3) were prepared according to our previous applied method [50, 52]. These reactions proceeded by their relative thiazoles, iodine and thiourea in presence of warm water (Scheme 1).



Scheme 1. Synthesis of the diamine monomers (DA-1-3).

3.2. Polymer synthesis and characterization

The aim of this research was introducing thiazole-based PIMs with high thermal and thermo-oxidative stability and CO₂ uptake capability. To achieve our goal, PIMs were synthesized by direct polycondensation of prepared diamine monomers with some aromatic dialdehydes. This reaction proceeds in the presence of LiBr as catalyst and freshly dried NMP as a solvent in 120 °C for 3 h and production of water as the only side-product (Scheme 2).



Scheme 2. Synthesis of the thiazole-containing PIMs-1-9.

As summarized in Table 1, PIMs were obtained in high yields (74–89%) with inherent viscosities in the range of 0.98–1.33 dL g⁻¹ in DMF solution at 30 °C, indicating high molecular weight of the synthesized PIMs. The highest efficiency of polymerization ascribed to the more linear structure of terephthalaldehyde and its less steric effect. Comparing other dialdehydes, 2,5-thiophenedicarboaldehyde, as a heterocyclic dialdehyde, shows better efficiency vs isophthalaldehyde causing by its more active structure. Furthermore, the reaction is affected by the type of applied primary acetophenone which arranges as follow: 3-nitroacetophenone>2-acetylnaphthalene>4'-bromoacetophenone.

Table 1. Synthetic conditions and inherent viscosities of PIMs.

Polymer Code	Ar	Ar'	NMP ^a (mL)	Yield ^b (%)	η_{inh}^c (dL/g)
PIM-1	3-nitrophenyl	(1)	2+1	89	1.28
PIM-2	3-nitrophenyl	(2)	2	82	1.09
PIM-3	3-nitrophenyl	(3)	2	87	1.17
PIM-4	4-bromophenyl	(1)	2+1	85	1.33
PIM-5	4-bromophenyl	(2)	2	74	1.11

PIM-6	4-bromophenyl	(3)	2	80	1.25
PIM-7	2-naphthyl	(1)	2+1	87	1.20
PIM-8	2-naphthyl	(2)	2	80	0.98
PIM-9	2-naphthyl	(3)	2+1	85	1.02

^a Amount of each DA and dialdehyde monomer = 1.0 mmol; reaction temperature 120 °C; reaction time 3 h. “2+1” means that an initial amount of 2 mL NMP was used and an additional 1 mL of NMP was added when the reaction solution became too viscous.

^b Isolated yield of PIM from corresponding DA.

^c Measured at a concentration of 0.5 g dL⁻¹ in DMF at 30 °C.

This order corresponds to the reaction mechanism that is largely dependent on the initial step of monomer synthesis, in which thiourea attacks to acetophenone derivatives via S_N² mechanism, and the more e-withdrawing substitution on acetophenone ultimately leads to improved yields. The data of elemental analysis for the proposed structure of the resulting PIMs were in good agreement with the calculated ones.

The FT-IR spectra of PIMs revealed the characteristic absorption bands for the imine C=N and aromatic C=C bonds stretching at ~ 1600-1675 cm⁻¹, and N-H stretching of amine groups at ~ 3341-3436 cm⁻¹. Absorption of aldehyde carbonyl stretching (C=O) end groups of polymers appears at 1699-1710 cm⁻¹. The typical FT-IR spectra of PIM-1-3 are shown in Figure 2.

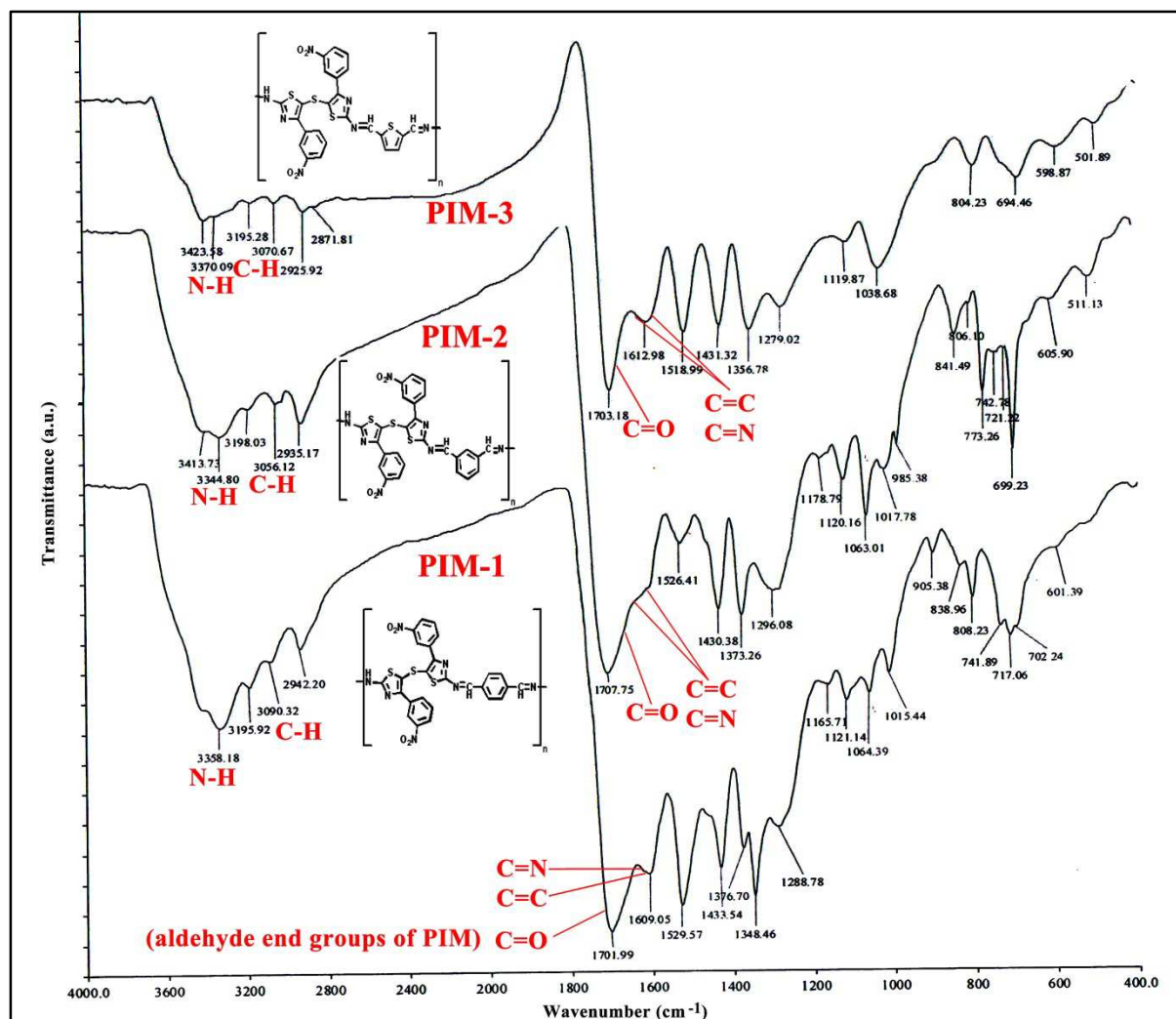


Figure 2. FT-IR spectra of PIM-1-3.

3.3. Polymer solubility

Solubility behavior was known as a key indicator to determine the morphology, processability and performance of the polymer in different applications such as gas separation membrane [58-60], printed electronics [61], solvent casting or immersion lithography [62, 63] and thin film for polymeric solar cells [64]. Furthermore, based on the literature, templating roles of solvent directing the pore size of polymers with its close dimension were reported [65]. On the other hand, solvent properties including its polarity, volatility and specific interaction features with the polymer material plays a pivotal role on degree of polymerization (DP), surface area, porosity and subsequently on CO₂ uptake capacity and

selectivity of polymer. In this sense, high boiling point and polarity solvents such as DMSO and DMF vs low polar solvents (dioxane, mesitylene) may result in high-polymerized and porous polymer by reducing the amount of entanglements and improving fractional free volume during the synthesis process [36]. It is also noteworthy that the mentioned solvent effect is more influential on the highly porous polymers with high-surface area. Hence, thiazole-containing PIMs were certified by dissolving 0.05 g of polymers in 1 mL of solvent for 24 h at rt (25 °C) or upon heating in tightly closed vials. As shown in Table S1 (supporting information), polymers represented excellent solubility in polar solvents including DMSO, DMF, DMAc, NMP, and pyridine at ambient temperature, and moderate solubility in THF and acetone. These findings are in accordance with synergic effects of flexible thioether units in the backbone with non-coplanar conformation and bulky pendants segments, phenyl and naphthyl substituents, which result in weakening of H-bonding and decreasing in close packing of polymer. However, the solubility of polymers was greatly dependent to the type of aldehydes used in polymerization processes. From this perspective, 2,5-thiophenedicarboaldehyde as an initial heteroaromatic dialdehyde in the synthesis of PIM-3 and PIM -6, causes insolubility of these polymers in THF solvent. In contrast to other aldehydes, it is completely compatible with the corresponding dialdehyde polar structure. Moreover, in the case of naphthyl-related polymers (PIM-7, PIM-8 and PIM-9) relatively better solubility was observed in less polar solvents including acetone and chloroform. This simultaneously is associated with the intrinsic effect of the non-polar pendent naphthyl group and its bulkiness through boosting detachment of polymer chains, and subsequently disrupting regularity and dense chain packing efficiency.

3.4. X-ray diffraction of the polymers

Wide-angle X-ray diffraction (WAXD) patterns were utilized for investigating the morphological aspects of the PIMs in a spectral window ranging from $2\theta = 4^\circ$ to 80° .

In general, the behavior of polymers can better be understood in terms of crystallinity of polymers which depend on the molecular and geometrical structure. On the other hand, bulk polymers with branches or irregular pendant groups (such as phenyl and naphthyl) are not completely crystalline as the value of entropy increases by more freely movement of the chains while pushing or pulling the polymer, and subsequently have a random molecular structure. This means amorphous polymers have no rigidity and sharp melting point, and exhibit flexibility and elasticity with impact resistance which are penetrated more by solvents than their crystalline counterparts. These features make amorphous polymers right choice for many industrial applications which need flexibility.

As shown in Figure 3, the amorphous nature of PIMs were confirmed due to broad curves without any obvious peak. This feature of polymers is mostly related to the presence of the pendent groups in the polymer backbone as the symmetry and regularity of backbone decreases by incorporation of bulky groups. It should be noted that these conditions occurs by weakening intermolecular forces such as H-bonding between the polymer chains and lowering chain packing efficiency which leads to decrease in crystallinity.

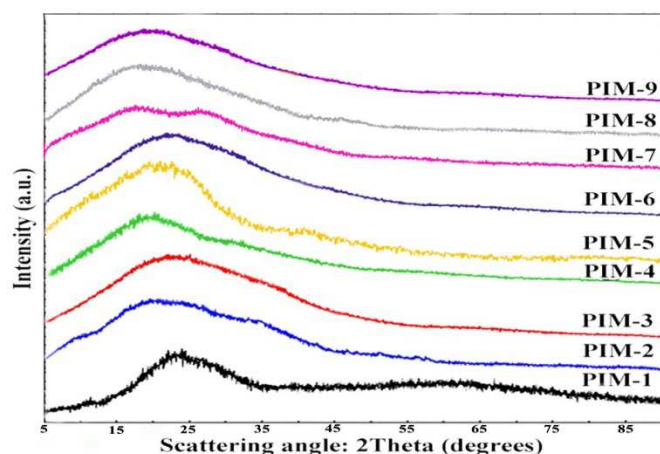


Figure 3. WAXD pattern of PIMs.

3.5. Thermal properties

The thermal properties of PIMs were investigated by DSC and TGA methods. The DSC analysis of the PIMs obviously confirmed full amorphous natures of polymers without any tendency to crystallize, even in the cooling step, as no evidence of crystallization and melting processes displayed. It is noteworthy that these data are fully consistent with the XRD results. As shown in Table 2, T_g values of the PIMs were in the range of 104–189 °C and directly affected by applied dialdehydes and initial diamines. Based on these data, increasing of T_g is a function of decreasing in flexibility of the PIM structure. In this regard, PIM-1, PIM-4 and PIM-7 exhibited higher T_g values, compared to respective homologous *meta*-substitution (PIM-2, PIM-5 and PIM-8), due to the rigid structure of polymer caused by 1,4-phenylene segments. While polymers PIM-7, PIM-8 and PIM-9 exhibited less T_g owing to their bulky naphthyl groups on polymer backbone, which increases the free volume between the polymer chains and greater flexibility. The main criteria to determine the thermal stability of polymers is the temperatures for 10% weight loss (T_{10}).

Table 2. Thermal characterizations of PIMs.

Polymer Code	DSC T_g^a (°C)	TGA		Char Yield ^c (%)
		Decomposition Temperature (°C)		
		In Air	In Nitrogen	
PIM-1	184	345	387	58
PIM-2	170	333	377	63
PIM-3	161	329	372	53
PIM-4	189	390	430	65
PIM-5	172	376	420	63
PIM-6	163	372	415	60
PIM-7	129	285	328	60
PIM-8	112	274	316	46
PIM-9	104	268	310	47

^a T_g Measured by DSC at scanning rate of 10 °C min⁻¹ in flowing nitrogen. ^b Temperature of 10% weight loss determined in N₂ and air atmospheres. ^c Residual weight (%) at 700 °C in N₂.

The T_{10} values of the PIMs were in the range of 310–430 °C in N₂ and 268–390 °C in air, respectively. The TGA-curves of the PIMs in N₂ atmosphere are shown in Figure 4 as well.

Accordingly, produced PIMs showed good thermal stability without notable weight loss below 310 °C in N₂ atmosphere. These evidences proved that PIMs do have thermal and oxidative resistances despite of their flexible thioether linkages and pendant phenyl or naphthyl groups.

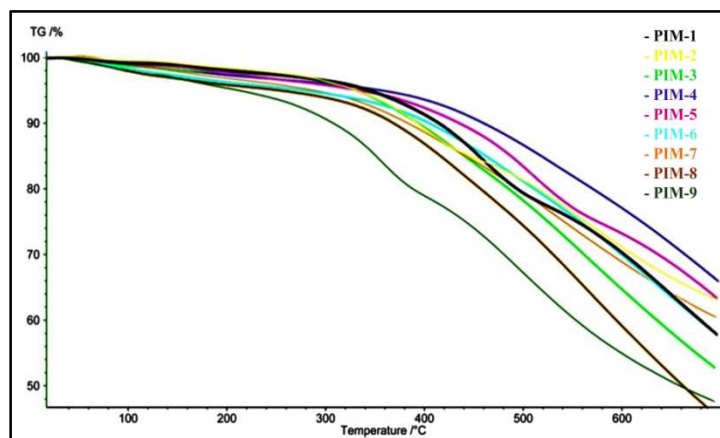


Figure 4. TGA-curves of the PIMs with a heating rate of 10 °C min⁻¹ in N₂ atmosphere.

3.6. BET analysis

In this study, non-coplanar conformation of PIMs and presence of bulky pendant segments (phenyl, naphthyl) in the polymer backbone resulted in decrease of intermolecular H-bonding and close packing of polymer and this may provide a proper condition for creating small pores among polymer chains to trap CO₂ gas. In addition, the PIMs comprising both rigid groups (benzene rings) and flexible linkages (thioether and C-C single bonds) lead to irregular pores due to the random orientation of flexible linkages. Therefore, N₂ adsorption-desorption measurements at 77 K were performed to determine the porosity and specific surface area of polymers. As illustrated in Figure 5 (a), the linear PIM-1 and PIM-4 exhibited a type-III isotherm, according to the IUPAC classification, with slit-shaped pore characteristic. Other PIMs revealed type-IV N₂ isotherm with H3 and H4 hysteresis loops and cylindrical and conical like pore shapes which was indicative of mesopores. The textural properties of PIMs are presented in Table 3. The minor surface areas were obtained, for PIM-

1 ($S_{\text{BET}} = 50.3 \text{ m}^2/\text{g}$) and PIM-4 ($S_{\text{BET}} = 56.1 \text{ m}^2/\text{g}$) by applying the BET model which correspond to compact linear polymer structure. On the other hand, PIM-7 has the highest level of surface area ($S_{\text{BET}} = 507.9$) which is consistent with presence of regular repetition of bulky naphthyl groups and structure of polymer chains. The pore size distribution (PSD) was estimated on the basis of BJH model, and determined most of the pores in mesoporous region (2-50 nm, Figure 5 (b)).

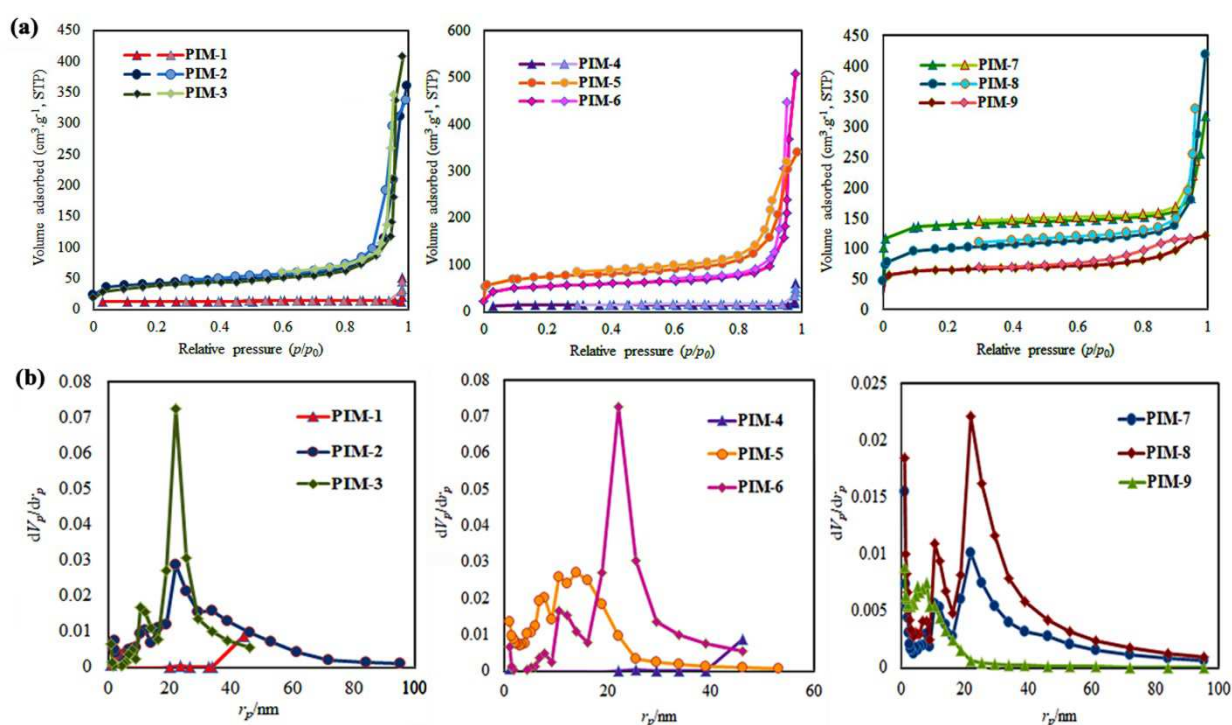


Figure 5. (a) N_2 adsorption/desorption isotherms and pore size distributions of PIMs at 77 K. (b) pore size distributions of PIMs.

Table 3. Textural properties of the PIMs.

Polymer Code	S_{BET}^a (m^2/g)	$V_p^{a,b}$ (cm^3/g)	$D_{p, \text{BJH}}^{a,c}$ (nm)
PIM-1	50.3	0.054	6.1
PIM-2	149.4	0.50	7.4
PIM-3	103.6	0.63	14.3
PIM-4	56.1	0.071	6.7
PIM-5	272.7	0.44	7.7
PIM-6	198.5	0.73	15.8
PIM-7	507.9	0.28	3.7
PIM-8	378.5	0.50	6.6
PIM-9	241.8	0.10	3.1

^a The parameters were measured by N_2 adsorption at 77 K.

^b Total pore volume at $P/P_0 = 0.99$.

^c Average pore diameter.

3.7. CO₂ uptake

The synthesized and characterized PIMs were subjected to CO₂ absorption experiments. Initially, all polymers were tested at rt (298 K and 1 bar) by using a laboratory setup for CO₂ capturing. The CO₂ absorptions of all polymers were determined in mmol or mg of CO₂ per gram of PIM value (mmol g⁻¹_{PIM} or mg g⁻¹_{PIM}). The results of absorption-desorption experiments are shown in Figure 6.

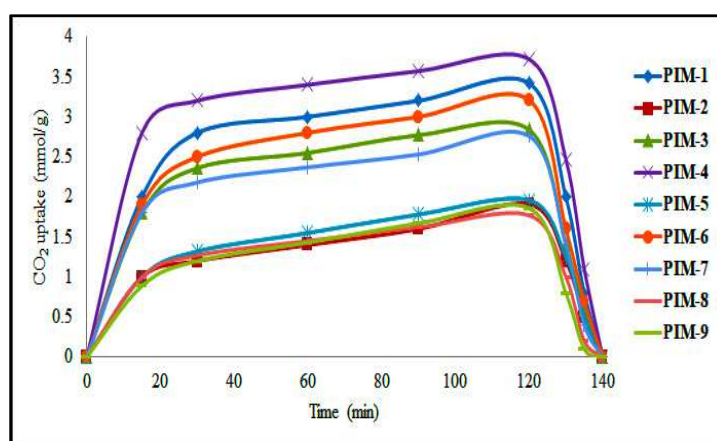


Figure 6. CO₂ absorption-desorption of PIMs; absorptions (at 298 K and 1 bar) and desorptions (at 373 K under vacuum condition (100 m bar) for 15 min).

As can be observed, the absorption reaches to its maximum amount in 120 min and complete desorption in 20 min. Furthermore, the CO₂ absorption diagrams revealed that the amount of polymers absorptions display a higher growth rate in the first 30 minutes of the experiment, due to the active sites on polymers, and after occupying some of those active points, the CO₂ absorption continues at a more balanced rate in the next few minutes. The prepared PIMs, as a type of nitrogen-rich Schiff-base including dipolar thiazole-based heterocycle, would make favorably interact with CO₂ molecules through dipole-quadrupole interactions and H-bonds (Scheme 3). As seen in Table 4, the PIMs prepared with incorporation of terephthalaldehyde exhibited more favorable CO₂ capturing compared with their isophthalaldehyde derivative ones. Despite low porosity and surface area of linear PIM-1 (3.42 mmol/g, 150.48 mg/g, $S_{\text{BET}} = 50.3 \text{ m}^2/\text{g}$) and PIM-4 (3.72 mmol/g, 163.68 mg/g, $S_{\text{BET}} = 56.1 \text{ m}^2/\text{g}$), their high gas

absorption is associated with reduction of polymer agglomeration and steric effects, which might result in a more degree of polymerization (DP) and repetitive set of efficient functional groups. However, a survey for a range of materials (including COFs, MOPs, MOFs and BPL carbon) revealed that increasing in BET surface area is not determining factor and a proper strategy for enhancing CO₂ uptake at lower pressures (1 bar) [31]. Furthermore, CO₂ sorption values for PIM-1 and PIM-4 are comparable to the previously reported porous polymers at 1 bar such as TH-COF-1 (97 mg/g, 2.2 mmol/g, $S_{\text{BET}} = 684 \text{ m}^2/\text{g}$ at 298 K) [28]; [HO₂C]_{100%}-H₂P-COF (76 mg/g, $S_{\text{BET}} = 364 \text{ m}^2/\text{g}$ at 298 K) [30]; MOP-C (2.2 mmol/g, $S_{\text{BET}} = 1237 \text{ m}^2/\text{g}$ at 298 K) [31]; DBF (2.2 mmol/g, $S_{\text{BET}} = 661 \text{ m}^2/\text{g}$ at 298 K) [33]; CMOP-1 (1.85 mmol/g, $S_{\text{BET}} = 431 \text{ m}^2/\text{g}$ at 273 K) [34]; FPOP-2 (1.31 mmol/g, $S_{\text{BET}} = 954 \text{ m}^2/\text{g}$ at 298 K) [41]. The increased CO₂ uptake in linear PIM-7 (121.44 mmol/g, $S_{\text{BET}} = 50.3 \text{ m}^2/\text{g}$) could be related to the gap between the polymer chains via bulk naphthyl group and subsequently increasing its specific surface area as well. It is also interesting that the PIMs using 2,5-thiophenedicarboxaldehyde showed relatively more CO₂ uptake, in spite of their lower surface area than the PIMs synthesized with isophthalaldehyde. This is probably related to sulfur atom on heterocyclic structure of dialdehyde and possibility of interaction between the non-bonding electrons of sulfur with a CO₂ molecule which can provide a stable six-membered ring (as shown in Scheme 3). In addition, the bulky aromatic group of "2-naphthyl" in PIM-7, PIM-8 and PIM-9 exhibited less CO₂ absorption, compared to their respective homologous ("3-nitrophenyl" and "4'-bromophenyl"), due to detachment of polymer chains which lead to disrupting regularity and dense chain packing efficiency, increasing steric barrier for CO₂ molecule approaching to these polymers, and absence of influential -NO₂ and -Br functional groups. These results highlight the positive and influential effect of functionalization (chemisorption) vs the specific surface area (physisorption) of polymers in terms of CO₂ uptake. Interestingly, more CO₂ capturing of PIM-4 (163.68 mg/g,

PIM-8	1.77	77.88	0.35	15.5	55	6.2
PIM-9	1.86	81.84	0.44	19.36	57	7
DA-1	1.40	61.6	-	-	-	-
DA-2	1.48	65.12	-	-	-	-
DA-3	1.37	60.28	-	-	-	-

In continuation, effects of temperature and pressure were investigated. As depicted in Figure 7, increasing temperature from 298 K to 318 K, which means increase in kinetic energy of CO₂ molecule along with increasing polymer mobility especially by thiourea bridge, causes weakening of CO₂ interaction with amine and imine groups on polymers, and subsequently reduction in the amount of absorbed CO₂ molecules. In contrast, increase in pressure results in gas density enhancement and consequently more gas absorption.

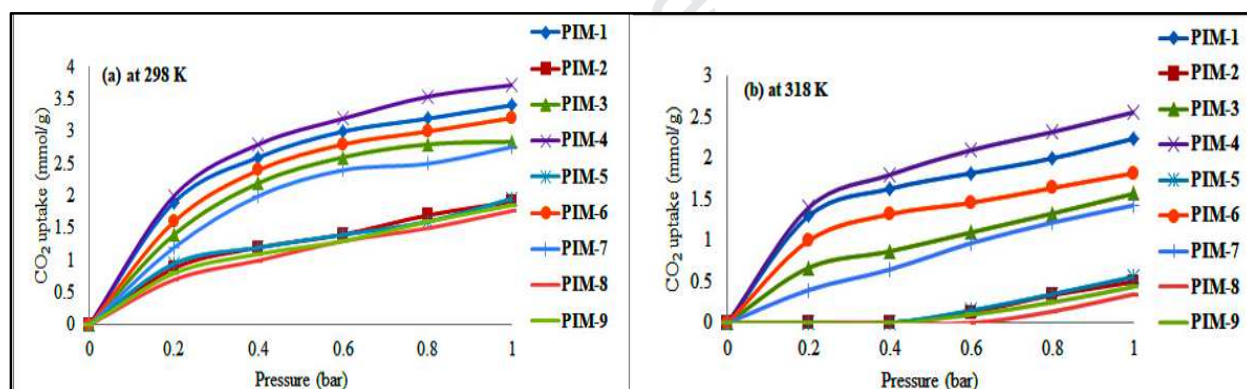


Figure 7. CO₂ absorption of PIMs at (a) 298 K and (b) 318 K.

Since regeneration of polymers for CO₂ experiment are valuable issue for gas separation, we continued our studies with typical PIM-4 in order to evaluate the polymer recycling capability for CO₂ absorption. In this regard, we examined the polymer to another CO₂ uptake to determine its reversibility after the first absorption-desorption analysis. It was found that the PIM-4 can properly be recovered for at least seven cycles without noticeable loss in efficiency (Figure 8). In addition to the CO₂ absorption capacity and reversibility, CO₂ selectivity of PIMs over N₂ and CH₄ was studied at 298 K up to 1 bar.

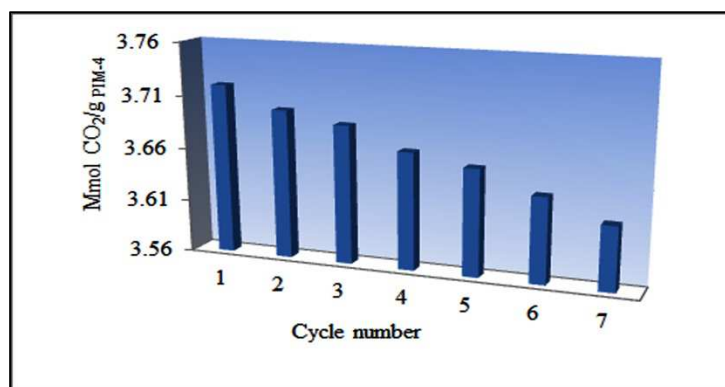


Figure 8. Recycling absorption of CO₂ over PIM-4.

The diagrams are displayed in Figure 9, in which PIM-4 and PIM-1, respectively, exhibited higher ideal selectivity ratios (CO₂/N₂: 77.3, 70.2 and CO₂/CH₄: 13.7, 12.5) among polymers by virtue of their linear packed structure resulting greater affinity toward CO₂. Moreover, the PIMs with naphthalene groups, particularly PIM-8 and PIM-9, revealed lowest gas selectivity ratios (CO₂/N₂: 55, 57 and CO₂/CH₄: 6.2, 7 respectively). This is because of increasing the polymer chains distance by presence of bulky naphthyl groups along with increasing steric effects, which leads to a decrease in effective interaction of gas and polymer, and reducing the selectivity of these polymers as a result. As shown in Table S2, a comparison of CO₂ absorption and selectivity of PIMs with various polymers such as benzimidazole-linked polymers (BILPs) [37-40], hyper-cross-linked heterocyclic MOPs [33], and imine-linked 2D-COFs [28, 30] were investigated which introduces PIMs as promising candidates for CO₂ uptake and selectivity.

The FT-IR spectroscopy was applied for comparison before and after CO₂ absorption on polymers. As illustrated in FT-IR spectra of PIMs-1-9 in Figures S10-27, the polymers exposed to CO₂ exhibited characteristic broad and strong absorption band at 3331-3431 cm⁻¹ for N-H and imine C-H stretching vibrations, which display a shift toward lower frequencies due to the H-bonding with CO₂ compared to corresponding not gas affected polymer. The aromatic C-H stretching vibrations were emerged in the range of 2929-3199 cm⁻¹. The PIMs

were also featured by strong absorption band at 1700-1708 cm^{-1} for C=O stretching of carbamate moiety, which was formed from the interaction of non-bonding electrons of imine with CO_2 molecule.

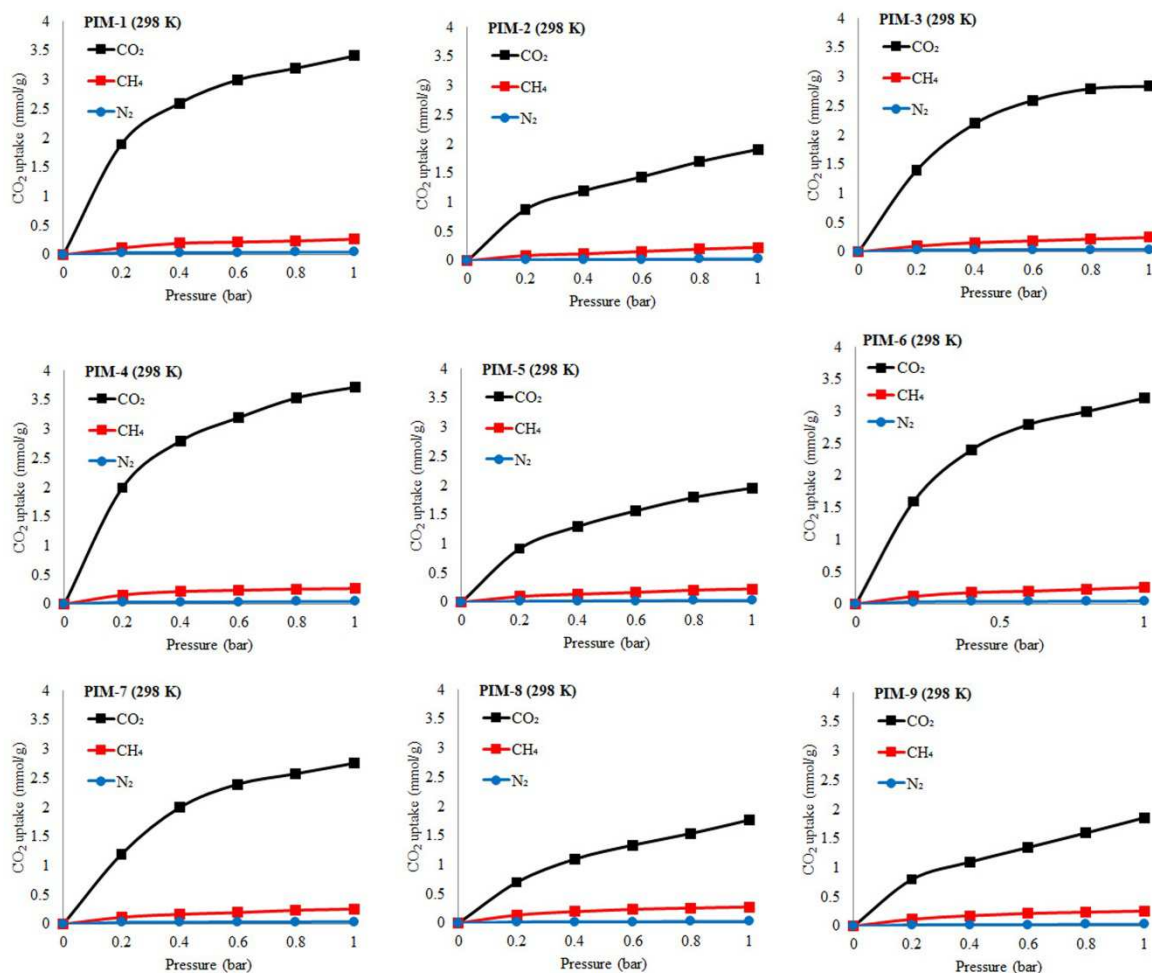


Figure 9. Selective gas (CO_2 , CH_4 , N_2) absorptions for PIMs at 298 K.

However, the absorption of aldehyde carbonyl groups at two end sides of polymer chain was overlapped in carbonyl area. A broad stretching vibration band at $\sim 1602\text{-}1627 \text{ cm}^{-1}$ related to aromatic C=C and imine C=N bonds. The FT-IR spectra of typical PIM-7, before and after CO_2 absorption, have shown in Figure 10. These results clearly prove the formation of H-

bonding of polymer with CO₂ molecules which is consistency with the proposed mechanism for CO₂ absorption on PIMs in Scheme 3.

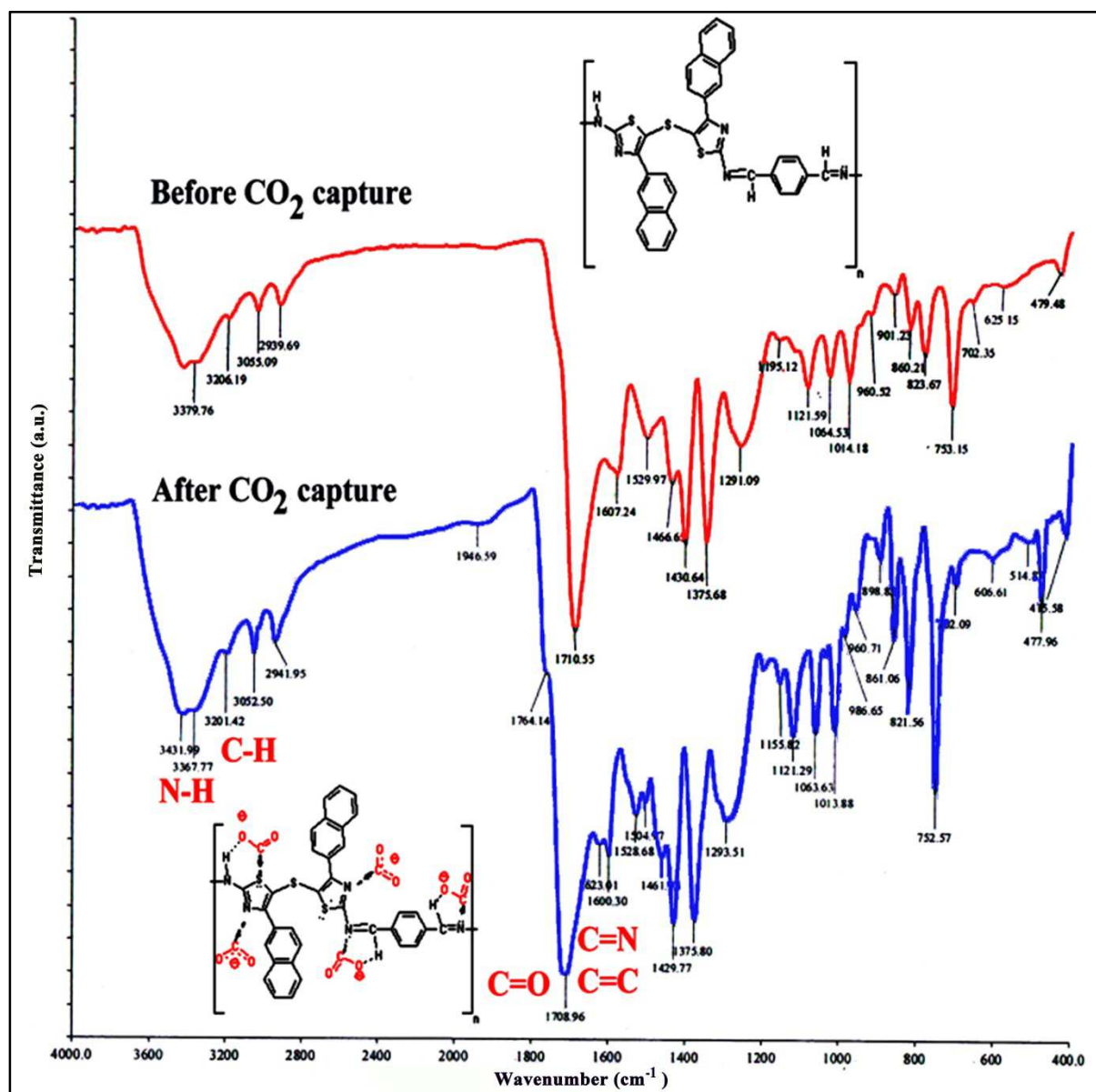


Figure 10. Comparative FT-IR spectra before and after CO₂ uptake of PIM-7.

4. Conclusion

In conclusion, nine non-coplanar *ortho*-linked thiazole-based PIMs with thioether linkage were synthesized as efficient chemical absorbents for CO₂ capturing with decent solubility, processability, thermal stability, low cost and non-toxicity. The PIMs were characterized by

viscosity, FT-IR, XRD, BET, elemental and thermal analysis. Based on abundant and robust polymeric imine groups and sulfur contents of thiazole heterocyclic ring in polymer structure, they successfully exhibited very high CO₂ absorption (particularly linear PIM-1 and PIM-4, 3.42 and 3.72 mmol g⁻¹) along with excellent ideal selectivity (up to CO₂/N₂: 77.3 and CO₂/CH₄: 13.7) at ambient condition. These results revealed a correlation between high selectivity and high CO₂ uptake among utilized PIMs. The amount of CO₂ absorption and ideal selectivity explained by synergistic physically, chemically and structurally aspects of PIMs and non-polarizable structures of N₂ and CH₄ compared with CO₂ molecule. Recycling absorption of PIM-4 proved no significant loss of CO₂ uptake efficiencies after 7 cycles. Gas absorption comparison of these polymers with their initial diamines was sufficient evidence for significant influence of polymerization process on these materials. Resulted experiments approved the consequences of increasing pressure and reducing temperature in increasing the rate of polymers gas absorption. Impression of structure and substitution on polymers were explored and it was found that the best results belongs to linear and packed polymers with less steric barriers in terms of thermal resistance and CO₂ absorption. These PIMs with high chemical and thermochemical stabilities are considered as promising scaffolds by virtue of cost-effective and readily available monomers, high selectivity and reversibility in CO₂ capturing and usability in various industries (such as membranes) due to their non-corrosive, environmentally compatibility and processing capability. Further efforts to prepare various membranes of these PIMs are ongoing in our group, with the aim of efficient and selective gas separations.

Supporting information

The characterization data of DA-1-3 and PIMs-1-9 and comparison table of CO₂ uptake and selectivity for polymers.

Conflicts of interest

There are no conflicts to declare.

Acknowledgements:

This work was supported by the Iran National Science Foundation (INSF) [grant No. 96007054] and Kharazmi University. The authors gratefully acknowledge for financial support of researchers and elites of this project.

Journal Pre-proof

References

- [1] H. Kheshgi, H. de Coninck, J. Kessels, Carbon dioxide capture and storage: Seven years after the IPCC special report, *Mitig. Adapt. Strateg. Glob. Change*. 17 (2012) 563–567.
- [2] J. D. Figueroa, T. Fout, S. Plasynski, H. McIlvried, R. D. Srivastava, Advances in CO₂ capture technology—The U.S. Department of Energy's Carbon Sequestration Program, *Int. J. Greenh. Gas Control*. 2 (2008) 9-20.
- [3] M. T. Ho, G. Leamon, G. W. Allinson, D. E. Wiley, Economics of CO₂ and mixed gas geosequestration of flue gas using gas separation membranes, *Ind. Eng. Chem. Res.* 45 (2006) 2546-2552.
- [4] B. Li, Y. Duan, D. Luebke, B. Morreale, Advances in CO₂ capture technology: A patent review, *Appl. Energ.* 102 (2013) 1439-1447.
- [5] B. Dutcher, M. Fan, A. G. Russell, Amine-Based CO₂ Capture Technology Development from the Beginning of 2013-A Review, *ACS Appl. Mater. Interfaces*. 7 (2015) 2137-2148.
- [6] Sh. Zeng, X. Zhang, L. Bai, X. Zhang, H. Wang, J. Wang, D. Bao, M. Li, X. Liu, S. Zhang, Ionic-liquid-based CO₂ capture systems: structure, interaction and process, *Chem. Rev.* 117 (2017) 9625-9673.
- [7] M. Aghaie, N. Rezaei, S. Zendejboudi, A systematic review on CO₂ capture with ionic liquids: Current status and future prospects, *Renew. Sust. Energ. Rev.* 96 (2018) 502-525.
- [8] R. Ben-Mansour, M. A. Habib, O.E. Bamidele, M. Basha, N. A. A. Qasem, A. Peedikakkal, T. Laoui, M. Ali, Carbon capture by physical adsorption: Materials, experimental investigations and numerical modeling and simulations-A review, *Appl. Energ.* 161 (2016) 225-255.

- [9] B. R. Pimentel, A. Parulkar, E-K. Zhou, N. A. Brunelli, R. P. Lively, Zeolitic imidazolate frameworks: next-generation materials for energy-efficient gas separations, *ChemSusChem*. 7 (2014) 3202-3240.
- [10] B. Chen, Zh. Yang, Y. Zhu, Y. J. Xia, Zeolitic imidazolate framework materials: recent progress in synthesis and applications, *Mater. Chem. A*. 2 (2014) 16811-16831.
- [11] K. Sumida, D. L. Rogow, J. A. Mason, Th. M. McDonald, E. D. Bloch, Z. R. Herm, T-H. Bae, J. R. Long, Carbon dioxide capture in metal-organic frameworks, *Chem. Rev.* 112 (2012) 724-781.
- [12] Ch. A. Trickett, A. Helal, B. A. Al-Maythaly, Z. H. Yamani, K. E. Cordova, O. M. Yaghi, The chemistry of metal-organic frameworks for CO₂ capture, regeneration and conversion, *Nat. Rev. Mater.* 2 (2017) 17045.
- [13] Ch. Chen, S. Zhang, K. H. Row, W-S. Ahn, Amine-silica composites for CO₂ capture: A short review, *J. Energy Chem.* 26 (2017) 868-880.
- [14] K. S. Sánchez-Zambrano, L. L. Duarte, D. A. S. Maia, E. Vilarrasa-García, M. Bastos-Neto, E. Rodríguez-Castellón, D. C. S. Azevedo, CO₂ Capture with mesoporous silicas modified with amines by double functionalization: assessment of adsorption/desorption cycles, *Materials*. 11 (2018), 887.
- [15] Ch. Chen, S. Bhattacharjee, Mesoporous silica impregnated with organoamines for post-combustion CO₂ capture: a comparison of introduced amine types, *Greenhouse Gas Sci. Technol.* 7 (2017) 1116-1125.
- [16] G-L. Zhuang, M-Y. Wey, H-H Tseng, The density and crystallinity properties of PPO-silica mixed-matrix membranes produced via the in situ sol-gel method for H₂/CO₂ separation II: Effect of thermal annealing treatment, *Chem. Eng. Res. Des.* 104 (2015) 319-332.

- [17] G-L. Zhuang, H-H. Tseng, M-Y. Wey, Preparation of PPO-silica mixed matrix membranes by in-situ sol-gel method for H₂/CO₂ separation, *Int. J. Hydrogen Energy*. 39 (2014) 17178-17190.
- [18] T-H. Weng, H-H. Tseng, M-Y. Wey, Effect of SBA-15 texture on the gas separation characteristics of SBA-15/polymer multilayer mixed matrix membrane, *J. Membr. Sci.* 369 (2011) 550–559.
- [19] H-H. Tseng, P-T. Shiu, Y-Sh. Lin, Effect of mesoporous silica modification on the structure of hybrid carbon membrane for hydrogen separation, *Int. J. Hydrogen Energy*. 36 (2011) 15352-15363.
- [20] M. S. Shafeeyan, W. M. A. W. Daud, A. Houshmand, A. Shamiri, A review on surface modification of activated carbon for carbon dioxide adsorption, *J. Anal. Appl. Pyrolysis*. 89 (2010) 143–151.
- [21] Ch-H. Yu, Ch-H. Huang, Ch-S. Tan, A review of CO₂ capture by absorption and adsorption, *Aerosol Air Qual. Res.* 12 (2012) 745-769.
- [22] D. G. Madden, H. S. Scott, A. Kumar, K-J. Chen, R. Sani, A. Bajpai, M. Lusi, T. Curtin, J. J. Perry, M. J. Zaworotko, Flue-gas and direct-air capture of CO₂ by porous metal-organic materials, *Philos. Trans. R. Soc. A*. 375 (2017) 20160025.
- [23] Q. Wang, J. Luo, Z. Zhong, A. Borgna, CO₂ capture by solid adsorbents and their applications: current status and new trends, *Energy Environ. Sci.* 4 (2011) 42-55.
- [24] J. Ahmad, W. U. Rehman, K. Deshmukh, Sh. Kh. Basha, B. Ahamed, K. Chidambaram, Recent advances in poly (amide-b-ethylene) based membranes for carbon dioxide (CO₂) capture: a review, *Polym. Plast. Technol. Eng.* 58 (2019) 366-383.
- [25] V. S. P. K. Neti, X. Wu, Sh. Deng, L. Echegoyen, Selective CO₂ capture in an imine linked porphyrinporous polymer, *Polym. Chem.* 4 (2013) 4566-4569.

- [26] J. Wang, I. Senkowska, M. Oschatz, M. R. Loheh, L. Borchardt, A. Heerwig, Q. Liu, S. Kaskel, Highly porous nitrogen-doped polyimine-based carbons with adjustable microstructures for CO₂ capture, *J. Mater. Chem. A*. 1 (2013) 10951-10961.
- [27] A. Rossin, G. Tuci, G. Giambastiani, M. Peruzzini, 1D and 2D Thiazole-based copper(II) coordination polymers: synthesis and applications in carbon dioxide capture, *ChemPlusChem*. 79 (2014) 406-412.
- [28] L. Wang, B. Dong, R. Ge, F. Jiang, J. Xiong, Y. Gao, J. Xu, A thiadiazole-functionalized covalent organic framework for efficient CO₂ capture and separation, *Microporous Mesoporous Mater.* 224 (2016) 95-99.
- [29] D. Kaleeswaran, P. Vishnoi, R. Murugavel, [3+3] Imine and β -ketoenamine tethered fluorescent covalent-organic frameworks for CO₂ uptake and nitroaromatic sensing, *J. Mater. Chem. C*. 3 (2015) 7159-7171.
- [30] N. Huang, X. Chen, R. Krishna, D. Jiang, Two-dimensional covalent organic frameworks for carbon dioxide capture through channel-wall functionalization, *Angew. Chem. Int. Ed.* 54 (2015) 2986-2990.
- [31] R. Dawson, E. Stöckel, J. R. Holst, D. J. Adams, A. I. Cooper, Microporous organic polymers for carbon dioxide capture, *Energy Environ. Sci.* 4 (2011) 4239-4245.
- [32] Z. Chang, D-Sh. Zhang, Q. Chen, X-H. Bu, Microporous organic polymers for gas storage and separation applications, *Phys. Chem. Chem. Phys.* 15 (2013) 5430-5442.
- [33] M. Saleh, H. M. Lee, K. CH. Kemp, K. S. Kim, Highly stable CO₂/N₂ and CO₂/CH₄ selectivity in hyper-cross-linked heterocyclic porous polymers, *Appl. Mater. Interfaces*. 6 (2014) 7325-7333.
- [34] J-R. Song, W-G. Duan, D-P. Li, Synthesis of nitrogen-rich polymers by click polymerization reaction and gas sorption property, *Molecules*. 23 (2018) 1732.

- [35] Ch. Xu, Z. Bacsik, N. Hedin, Adsorption of CO₂ on a micro-/mesoporous polyimine modified with tris(2-aminoethyl)amine, *J. Mater. Chem. A*, 3 (2015) 16229-16234.
- [36] N. Popp, Th. Homburg, N. Stock, J. Senker, Porous imine-based networks with protonated imine linkages for carbon dioxide separation from mixtures with nitrogen and methane, *J. Mater. Chem. A*, 3 (2015) 18492-18504.
- [37] A. K. Sekizkardes, S. Altarawneh, Z. Kahveci, T. İslamoglu, H. M. El-Kaderi, Highly selective CO₂ capture by triazine-based benzimidazole-linked polymers, *Macromolecules*, 47 (2014) 8328-8334.
- [38] M. G. Rabbani, H. M. El-Kaderi, Template-free synthesis of a highly porous benzimidazole-linked polymer for CO₂ capture and H₂ storage, *Chem. Mater.* 23 (2011) 1650-1653.
- [39] M. G. Rabbani, H. M. El-Kaderi, Synthesis and characterization of porous benzimidazole-linked Polymers and their performance in small gas storage and selective uptake, *Chem. Mater.* 24 (2012) 1511-1517.
- [40] M. G. Rabbani, T. E. Reich, R. M. Kassab, K. T. Jackson, H. M. El-Kaderi, High CO₂ uptake and selectivity by triptycene-derived benzimidazole-linked polymers, *Chem. Commun.* 48 (2012) 1141-1143.
- [41] X. Sun, Y. Qi, J. Li, W. Wang, Q. Ma, J. Liang, Ferrocene-linked porous organic polymers for carbon dioxide and hydrogen sorption, *J. Organomet. Chem.* 859 (2018) 117-123.
- [42] C. A. Scholes, Sh. Kanehashi, Polymer of intrinsic microporosity (PIM-1) membranes treated with supercritical CO₂, *Membranes*, 9 (2019) 41.
- [43] A. D. Regno, A. Gonciaruk, L. Leay, M. Carta, M. Croad, R. Malpass-Evans, N. B. McKeown, F. R. Siperstein, Polymers of intrinsic microporosity containing Tröger base for CO₂ capture, *Ind. Eng. Chem. Res.* 52 (2013) 16939–16950.

- [44] H. A. Patel, C. T. Yavuz, Noninvasive functionalization of polymers of intrinsic microporosity for enhanced CO₂ capture, *Chem. Commun.* 48 (2012) 9989-9991.
- [45] Ch-J. Sun, P-F. Wang, H. Wang, B-H. Han, All-thiophene-based conjugated porous organic polymers, *Polym. Chem.* 2016, 7, 5031-5038.
- [46] S. H. Je, O. Buyukcakir, D. Kim, A. Coskun, Direct utilization of elemental sulfur in the synthesis of microporous polymers for natural gas sweetening, *Chem.* 1 (2016) 482-493.
- [47] Y. Sun, J. Zhao, J. Wang, N. Tang, R. Zhao, D. Zhang, T. Guan, K. Li, sulfur-doped millimeter-Sized microporous activated carbon spheres derived from sulfonated poly(styrene-divinylbenzene) for CO₂ capture, *J. Phys. Chem. C.* 121 (2017) 10000-10009.
- [48] H. A. Patel, F. Karadas, J. Byun, J. Park, E. Deniz, A. Canlier, Y. Jung, M. Atilhan, C. T. Yavuz, Highly stable nanoporous sulfur-bridged covalent organic polymers for carbon dioxide removal, *Adv. Funct. Mater.* 23 (2013) 2270-2276.
- [49] A. Javadi, A. Shockravi, M. Kamali, A. Rafieimanesh, A. M. Malek, Solution processable polyamides containing thiazole units and thioether linkages with high optical transparency, high refractive index, and low birefringence, *Polym. Chem.* 51 (2013) 3505-3515.
- [50] A. Javadi, Z. Najjar, S. Bahadori, V. Vatanpour, A. Malek, E. Abouzari-Lotf, A. Shockravi, High refractive index and low-birefringence polyamides containing thiazole and naphthalene units, *RSC Adv.* 5 (2015) 91670-91682.
- [51] J. Rezania, A. Shockravi, M. Ehsani, V. Vatanpour, Novel polyimides based on diamine containing thiazole units with thioether linkage and pyridine as pendent group: Synthesis and characterization, *High Perform. Polym.* 30 (2017) 840-846.

- [52] A. Javadi, A. Shockravi, M. Koohgard, A. Malek, F. A. Shourkaei, S. Ando, Nitro-substituted polyamides: A new class of transparent and highly refractive materials, *Eur. Polym. J.* 66 (2015) 328-341.
- [53] A. Javadi, A. Shockravi, A. Rafieimanesh, A. Malek, S. Ando, Synthesis and structure–property relationships of novel thiazole-containing poly(amide imide)s with high refractive indices and low birefringences, *Polym. Int.* 64 (2015) 486-495.
- [54] A. Shockravi, A. Javadi, M. Kamali, S. J. Hajavi, Highly refractive and organo-soluble poly(amide imide)s based on 5,5'-thiobis(2-amino-4-methyl-thiazole): Synthesis and characterization, *Appl. Polym. Sci.* 125 (2012) 1521-1529.
- [55] E. Abouzari-Lotf, A. Shockravi, A. Rafieimanesh, M. Saremi, A. Javadi, M. M. Nasef, Novel polyoxadiazoles with non-coplanar *ortho*-linked structures as highly CO₂ permselective membranes, *RSC Adv.* 4 (2014) 17993-18002.
- [56] A. Shockravi, A. Olyaei, M. Sadeghpour, Synthesis of novel symmetrical bis-Schiff bases of 5,5'-methylenebis(2-aminothiazole), *J. Heterocyclic Chem.* 45 (2008) 1473-1475.
- [57] A. Shockravi, M. Sadeghpour, A. Olyaei, A convenient synthesis of novel symmetrical bis-Schiff bases of 2, 2'-thio-bis[4-methyl(2-aminophenoxy)phenyl ether] in solution and under solvent-free conditions, *J. Chem. Res.* 11 (2009) 656-658.
- [58] A. Ghadimi, S. Norouzbahari, V. Vatanpour, F. Mohammadi, An investigation on gas transport properties of cross-linked poly(ethylene glycol diacrylate) (XLPEGDA) and XLPEGDA/TiO₂ membranes with a focus on CO₂ separation, *Energy Fuels* 32 (2018) 5418–5432.
- [59] M. S. Ahmad, D. F. Mohshim, R. Nasir, H. A. Mannan, H. Mukhtar, Effect of solvents on the morphology and performance of Polyethersulfone (PES) polymeric membranes material for CO₂/CH₄ separation, *Mater. Sci. Eng.* 290 (2018) 012074.

- [60] R. Recio, L. Palacio, P. Prádanos, A. Hernández, Á. E. Lozano, Á. Marcos, J. G. de la Campa, J. de Abajo, Gas separation of 6FDA–6FpDA membranes Effect of the solvent on polymer surfaces and permselectivity, *J. Membrane Sci.* 293 (2007) 22–28.
- [61] H. Wang, B. Hsieh, G. Jiménez-Osés, P. Liu, C. J. Tassone, Y. Diao, T. Lei, K. N. Houk, Z. Bao, Solvent Effects on Polymer Sorting of Carbon Nanotubes with Applications in Printed Electronics, *Small*. 11 (2015) 11126-33.
- [62] E. L. Kendall, J. Y. Han, M. S. Wiederoder, A. Sposito, A. Wilson, O. D. Rahmanian, D. L. DeVoe, Soft lithography microfabrication of functionalized thermoplastics by solvent casting, *J. Polym. Sci., Part B: Polym. Phys.* 53 (2015), 1315–1323.
- [63] S. H. Nemati, D. A. Liyu, A. J. Canul, A. E. Vasdekis, Solvent immersion imprint lithography: A high-performance, semi-automated procedure, *Biomicrofluidics*. 11 (2017) 024111.
- [64] M.N. Yusli, T. Way Yun, K. Sulaiman, Solvent effect on the thin film formation of polymeric solar cells, *Mater. Lett.* 63 (2009) 2691–2694.
- [65] L-B. Sun, Y-H. Kang, Y-Q. Shi, Y. Jiang, X-Q. Liu, Highly selective capture of the greenhouse gas CO₂ in polymers, *ACS Sustainable Chem. Eng.* 3 (2015) 3077–3085.

Highlights

- New nine thiazole-based polyimines (PIMs) with thioether linkage are synthesized via simple Schiff-base condensation reaction.
- Polymers are characterized and structurally compared for CO₂ absorption-desorption and selectivity under ambient and high temperature conditions.
- CO₂ uptake of polymers is compared with their original diamines.
- Interaction mechanism of polymers and CO₂ molecule is investigated.